High-pressure sound velocities and elasticity of aluminous $MgSiO_3$ perovskite to 45 GPa: Implications for lateral heterogeneity in Earth's lower mantle

Jennifer M. Jackson,[1,2] Jianzhong Zhang,[3] Jinfu Shu,[4] Stanislav V. Sinogeikin,[1] and Jay D. Bass[1]

Received 23 May 2005; revised 15 September 2005; accepted 30 September 2005; published 3 November 2005.

[1] Brillouin scattering measurements on aluminous magnesium silicate perovskite, arguably the most abundant phase in Earth, have been performed to 45 GPa in a diamond anvil cell at room temperature, using methanol-ethanol-water and neon as pressure transmitting media. The experiments were performed on a polycrystalline sample of aluminous $MgSiO_3$ perovskite containing 5.1 ± 0.2 wt.% Al_2O_3. The pressure derivatives of the adiabatic bulk (K_{0S}) and shear (μ_{0S}) moduli are 3.7 ± 0.3 and 1.7 ± 0.2, respectively. These measurements allow us to evaluate whether the observed lateral variations of seismic wave speeds in Earth's lower mantle are due at least in part to a chemical origin. Our results indicate that a difference in the aluminum content of silicate perovskite, reflecting a variation in overall chemistry, is a plausible candidate for such seismic heterogeneity. **Citation:** Jackson, J. M., J. Zhang, J. Shu, S. V. Sinogeikin, and J. D. Bass (2005), High-pressure sound velocities and elasticity of aluminous $MgSiO_3$ perovskite to 45 GPa: Implications for lateral heterogeneity in Earth's lower mantle, *Geophys. Res. Lett.*, *32*, L21305, doi:10.1029/2005GL023522.

1. Introduction

[2] Accurate determinations of the sound velocities of deep Earth materials under the relevant pressures and temperatures are essential for understanding seismic observations in this region. For example, recent high-resolution seismic studies report large lateral velocity variations in Earth's lower mantle that cannot be explained by temperature alone and are probably caused by chemical variations [*Grand et al.*, 1997; *Ishii and Tromp*, 1999; *Masters et al.*, 2000; *Ni et al.*, 2002]. The nature of the chemical heterogeneity remains an open question for the geophysical community [*Trampert et al.*, 2004; *Mattern et al.*, 2005] and one that is challenging to address. Aluminum-bearing ferromagnesium silicate perovskite, ferropericlase, and calcium silicate perovskite (with Mg and Ca end-member formulae: $MgSiO_3$, MgO, and $CaSiO_3$, respectively) have been proposed to be the most abundant phases in Earth's lower mantle, with aluminous perovskite occupying roughly half of Earth's volume [*Anderson and Bass*, 1986; *Knittle and Jeanloz*, 1987; *Irifune*, 1994; *da Silva et al.*, 2000; *Fiquet et al.*, 2000; *Shim et al.*, 2000; *Wentzcovitch et al.*, 2004]. Despite its major role in the deep Earth, the sound velocities of aluminous perovskite at high-pressure have not been reported in the literature and therefore, have not been considered in recent attempts at interpreting seismic observations. Sound velocity measurements on aluminous silicate perovskite containing 5 wt.% Al_2O_3 under ambient conditions [*Jackson et al.*, 2004] showed that in comparison with $MgSiO_3$ perovskite [*Sinogeikin et al.*, 2004], the shear modulus decreases by about 6%, but the bulk modulus remains unchanged. Such a finding could have important implications for the interpretation of seismological observations in Earth's lower mantle.

[3] Previous experimental and theoretical studies have often yielded contradictory results on the question of whether the properties of magnesium silicate perovskite are significantly altered by the presence of Al^{3+} [*Zhang and Weidner*, 1999; *Brodholt*, 2000; *Andrault et al.*, 2001; *Daniel et al.*, 2001; *Yamamoto et al.*, 2003; *Akber-Knutsen and Bukowinski*, 2004; *Daniel et al.*, 2004; *Jackson et al.*, 2004; *Walter et al.*, 2004; *Yagi et al.*, 2004]. The effect of Al on the elastic properties may depend on the crystal-chemical details of how this ion is incorporated into the perovskite structure. This subtle but important complexity adds an additional element of uncertainty to the properties of the actual aluminous perovskite in the lower mantle. In this paper, we present measurements of the sound velocities of aluminous $MgSiO_3$ perovskite to lower mantle pressures and discuss their relevance to observed lateral seismic variations.

2. Experiment

[4] The polycrystalline aluminous $MgSiO_3$ perovskite sample (hereafter referred to as Al-Pv) was synthesized from a synthetic glass containing 80 mol% $MgSiO_3$ and 20 mol% $Mg_3Al_2Si_3O_{12}$ at 25 GPa and 1873 K for 2 hours in a 2000-ton Kawai-type multi-anvil apparatus. A portion of the run charge was polished to a platelet with parallel sides and a thickness of 40 μm for Brillouin measurements at ambient pressure [*Jackson et al.*, 2004] and then polished to a thickness of about 15 μm for the high-pressure measurements reported here. Electron microprobe analyses showed that the sample contains 5.1 ± 0.2 wt.% Al_2O_3, and an orthorhombic perovskite structure (*Pbnm*) was confirmed using powder X-ray diffraction (see *Jackson et al.* [2004] for more details).

[1]Department of Geology, University of Illinois, Urbana, Illinois, USA.
[2]Now at the Advanced Photon Source, Argonne National Laboratory, Argonne, Illinois, USA.
[3]Los Alamos National Laboratory, Los Alamos, New Mexico, USA.
[4]Carnegie Institution of Washington, Washington, D. C., USA.

0094-8276/05/2005GL023522$05.00

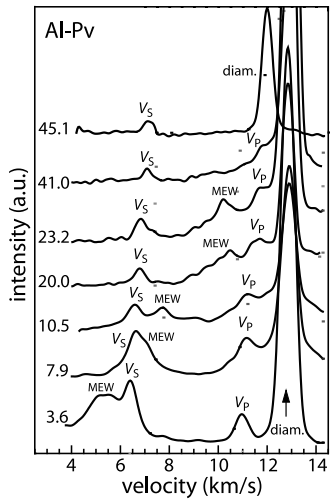

Figure 1. Selected Brillouin spectra of polycrystalline Al-Pv using different pressure transmitting media: methanol-ethanol-water (MEW) at $P = 3.6$, 7.9, 10.5, 20, 23.2, 41 GPa and neon at $P = 45.1$ GPa. The Brillouin peaks are labeled as follows: MEW, compressional (V_P) and shear (V_S) acoustic modes of Al-Pv, and the diamond shear acoustic mode (diam.) from both anvils.

[5] Three separate high-pressure Brillouin experiments on polycrystalline Al-Pv were performed in a 50 degree symmetric scattering geometry, using a symmetric piston-cylinder-type diamond anvil cell with a 60 degree full angle optical opening. An argon ion laser ($\lambda = 514.5$ nm) with a low input power was used (~30 mW focused to ~30 μm diameter onto the sample at pressures below 23 GPa, and ~55 mW at pressures greater than 23 GPa) in order to avoid any back-transformation of the Al-Pv sample to glass or enstatite. Details of the Brillouin scattering method [*Sandercock*, 1982] and layout design [*Sinogeikin et al.*, 1998] have been described previously. Before the samples were loaded, the opposing diamond anvils were rotated with respect to each other until the maximum shear velocities of the individual anvils were obtained. This configuration allowed for clear detection of the Al-Pv V_P Brillouin peak (see Figure 1). In each experiment, a different portion of the Al-Pv sample was loaded in an inconel or rhenium gasket, which was pre-indented to a thickness of about 50 μm. Ruby spheres [*Chervin et al.*, 2001] or chips were placed around the sample to serve as a pressure gauge, and methanol-ethanol-water (MEW) (16:3:1 by volume) or neon was used as a pressure-transmitting medium to ensure hydrostatic or quasihydrostatic conditions in the sample chamber. Uncertainties in pressure were determined from the standard deviation of the pressures calculated from the ruby fluorescence R_1 shift [*Mao et al.*, 1986] of several rubies within the sample chamber. To obtain good statistics on Brillouin peak intensities and positions, collection times for a single Brillouin run varied from 4 to 24 hours, and the DAC was rotated with respect to the incident laser beam between runs. Several representative spectra at different pressures are shown in Figure 1. When using MEW, pressure gradients within the sample chamber became apparent at around 13 GPa, as MEW freezes near this pressure. It is possible to alleviate the pressure gradients by annealing the DAC, but perovskite is metastable below ~23 GPa. To avoid any back transformation of the Al-Pv, the DAC was annealed in an oven for 4 hours at about 413 K at pressures greater than 23 GPa. Pressure gradients always decreased after annealing, and at the highest pressure achieved using MEW ($P = 41$ GPa), the pressure gradient was 0.7 GPa. In a separate set of experiments, neon was used as a pressure medium. Without annealing the neon, the pressure gradients were smaller than those measured in MEW at all pressures. At each pressure, the individual raw spectra were fit with a mixed Gaussian plus Lorentzian profile and the peak positions were recorded. The evaluated peak positions of all spectra at a given pressure were averaged. This average is the final velocity we report for a given pressure, and the associated uncertainties were calculated from the range of fitted peak positions at a given pressure (approximately 2σ) (Figure 2). For more experimental details, see *Jackson* [2005].

3. Results

[6] Using ambient pressure-temperature values of the adiabatic bulk modulus ($K_{0S} = 252 \pm 5$ GPa), shear modulus ($\mu_{0S} = 165 \pm 2$ GPa), and density ($\rho_0 = 4.081 \pm 0.002$ g/cm^3) for Al-Pv [*Jackson et al.*, 2004], the measured sound velocities as a function of pressure that are presented in Figure 2 were fit to a 3rd order finite-strain equation-of-state (EOS) [*Davies and Dziewonski*, 1975] to obtain $(dK_{0S}/dP)_T = K_S'$, $(d\mu_{0S}/dP)_T = \mu_S'$, and a set of best-fit densities at each pressure. A fit to all the data yields $K_S' = 3.7 \pm 0.3$ and $\mu_S' = 1.7 \pm 0.2$ (Figure 3). The calculated

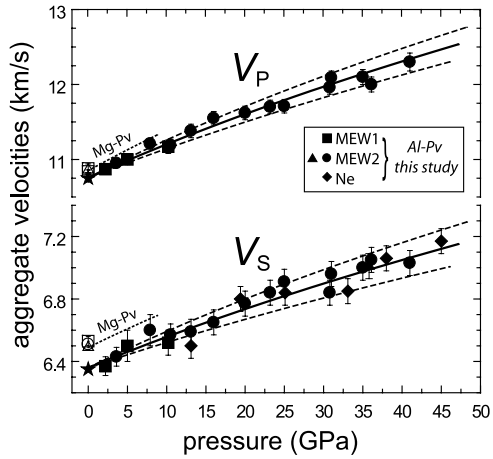

Figure 2. Aggregate sound velocities of polycrystalline Al-Pv from room pressure (stars, *Jackson et al.* [2004]) to 45 GPa. At high-pressure, the legend is as follows: sample loaded with MEW first run (MEW1) and second run (MEW2), sample loaded with neon (Ne), and data collected on decreasing pressure in MEW2 (filled triangle). The solid black lines are calculated from the best-fit elastic moduli (3rd order finite strain EOS), and the long-dashed lines represent the error determined from these fits. Sound velocity data for $MgSiO_3$ perovskite are as follows: *Sinelnikov et al.* [1998] (open circle), *Sinogeikin et al.* [2004] (open square), and *Li and Zhang* [2005] (open triangle and short-dashed line to 9.2 GPa). The uncertainties in pressure are less than the symbol size.

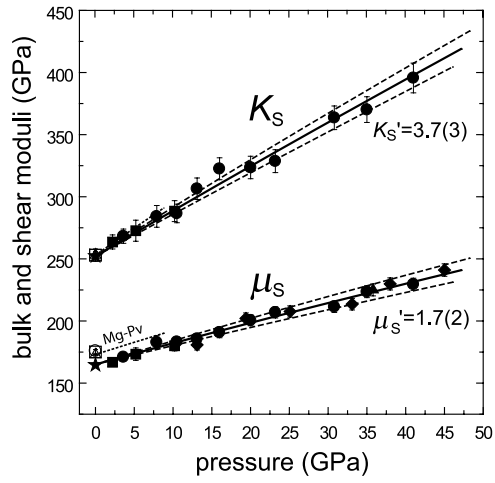

Figure 3. Aggregate elastic moduli of polycrystalline Al-Pv as a function of pressure. The symbols and lines have the same meaning as in Figure 2.

densities from this EOS were used to calculate K_S and μ_S at each pressure using the following relationships:

$$K_s = \rho\left(V_P^2 - \frac{4}{3}V_S^2\right)$$

$$\mu_S = \rho V_S^2$$

Standard error propagation was used to calculate the associated errors. Different pressure regions were also fit to the same EOS, including only the low pressure data where MEW is considered to be hydrostatic and the pressure region where Al-Pv is proposed to be stable. Although K_S' is more sensitive than μ_S' to these different regions of fit, no significant deviations were found.

[7] In an independent set of pressure-volume (*P-V*) X-ray diffraction measurements, a portion of Al-Pv from the same run charge used in this study yielded $(dK_{0T}/dP)_T = K_T' = 4.0 \pm 0.3$ and $K_{0T} = 251.5 \pm 2.7$ GPa [*Daniel et al.*, 2004], in agreement with the pressure derivative reported here and the bulk modulus reported by *Jackson et al.* [2004]. The isothermal bulk modulus from *Jackson et al.* [2004] ($K_{0T} = 250 \pm 5$ GPa) is also in agreement with *Ono et al.* [2004] (5 wt.% Al_2O_3, $K_{0T} = 256 \pm 9$ GPa, using the *Shim et al.* [2000] gold scale). However, our room-pressure bulk modulus is not in agreement with *Zhang and Weidner* [1999] (5 wt.% Al_2O_3, $K_{0T} = 234 \pm 2$ GPa), *Kubo et al.* [2000] (10 wt.% Al_2O_3, $K_{0T} = 198 \pm 27$ GPa), *Daniel et al.* [2001] (7.7 wt.% Al_2O_3, $K_{0T} = 229 \pm 4$ GPa and $K_T' = 2.5 \pm 0.4$), *Andrault et al.* [2001] (2.5 wt.% Al_2O_3, $K_{0T} = 266.7 \pm 2.8$ GPa), *Yagi et al.* [2004] (for 1.2, 5, and 10.3 wt.% Al_2O_3, $K_{0T} = 242$, 257, and 232 GPa, respectively), and *Walter et al.* [2004] (for 5.1, 9.8, 20.5, and 25.4 wt.% Al_2O_3, $K_{0T} = 268.9 \pm 7.0$, 262.6 ± 6.7, 254.2 ± 6.3, and 253.4 ± 6.2 GPa, respectively). In the above mentioned *P-V-(T)* studies K' was fixed to 4, unless otherwise mentioned.

[8] The sound velocities and elasticity of single-crystal and polycrystalline $MgSiO_3$ perovskite (hereafter referred to as Mg-Pv) have recently been reported using Brillouin scattering and show that the elastic moduli obtained by measurements of polycrystalline Mg-Pv agree with those obtained from the single-crystal data [*Sinogeikin et al.*, 2004] (see Figures 2 and 3). The shear properties of polycrystalline Mg-Pv at elevated *P-T* conditions were determined using ultrasonic interferometric techniques to 8 GPa and 800 K [*Sinelnikov et al.*, 1998], producing $\mu_S' = 1.8 \pm 0.4$. Using a similar technique and sample, simultaneous determination of V_P, V_S, and density of Mg-Pv were determined to 9.2 GPa and 873 K [*Li and Zhang*, 2005], producing $K_S' = 4.4 \pm 0.1$ and $\mu_S' = 2.0 \pm 0.1$. *P-V-T* measurements of Mg-Pv within its stability field (*P* up to 94 GPa and *T* up to 2900 K) obtained $K_T' = 3.69 \pm 0.04$ from the best fit thermal EOS [*Fiquet et al.*, 2000], a value that is equal to the K_S' value of 3.7 ± 0.3 obtained for Al-Pv in this study within the uncertainties.

4. Lateral Chemical Variations in the Lower Mantle

[9] Using the reported sound velocities of Mg-Pv at ambient conditions, *Jackson et al.* [2004] found that the relative variation of shear and compressional velocities, evaluated as $R = d\ln V_S/d\ln V_P$ [*Masters et al.*, 2000], as a function of aluminum content produces an *R* value of 2.3 at ambient conditions. Using the pressure derivatives (with associated uncertainties) obtained in this study for Al-Pv and the range of pressure derivatives from previous studies on Mg-Pv mentioned above, one can calculate a range of *R* values at a given pressure. At the highest pressure achieved in this study (*P* = 45 GPa, approximately 1150 km depth) *R* ranges from 1 to 4.5 for variations in aluminum content only, with values of *R* less than 2 obtained from using the higher pressure derivatives of Mg-Pv [*Li and Zhang*, 2005]. Seismological data suggest that *R* = 2.4 at equivalent depths [*Masters et al.*, 2000], a value within the range we calculate for aluminum variations in $MgSiO_3$ perovskite. Therefore, aluminum variations in silicate perovskite, thus reflecting overall chemistry changes in other lower mantle phases, cannot be ruled out as a possible source for lateral seismic variations. However, this agreement can be fortuitous. Athermal density functional theoretical calculations indicate that variations in iron content of silicate perovskite are unlikely to cause large lateral velocity variations, because an *R* value of only 1.6 was determined at 136 GPa [*Kiefer et al.*, 2002]. The chemical *R* values reported here and by *Kiefer et al.* [2002] do not reflect any lateral velocity variations that might be caused by temperature. Furthermore, it is unknown how the substitution of both iron and aluminum into $MgSiO_3$ perovskite would affect the sound velocities of end-member $MgSiO_3$ perovskite. Therefore, measurements of the sound velocities of aluminous ferromagnesium silicate perovskite at high-pressure and high-temperature are important, because it is possible that temperature variations combined with chemical variations in magnesium silicate perovskite may explain the observed large *R* values.

[10] **Acknowledgments.** We thank C. Sanchez-Valle, D. L. Lakshtanov, W. Sturhahn, and H.-K. Mao for helpful discussions. We thank the Geophysical Laboratory at the Carnegie Institute of Washington for providing access to their gas-loading facility and H. Hellwig for providing access to his Raman spectrometer. This research was funded by the NSF under grants EAR 0003383 and 0135642 and by the Mineralogical Society of America Grant for Student Research in Mineralogy and Petrology (JMJ).

References

Akber-Knutsen, S., and M. S. T. Bukowinski (2004), The energetics of aluminum solubility into $MgSiO_3$ perovskite at lower mantle conditions, *Earth Planet. Sci. Lett.*, *220*, 317–330.

Anderson, D. L., and J. D. Bass (1986), Transition region of the Earth's upper mantle, *Nature*, *320*, 321–328.

Andrault, D., N. Bolfan-Casanova, and N. Guignot (2001), Equation of state of lower mantle (Al, Fe)-$MgSiO_3$ perovskite, *Earth Planet. Sci. Lett.*, *193*, 501–508.

Brodholt, J. P. (2000), Pressure-induced changes in the compression mechanism of aluminous perovskite in Earth's mantle, *Nature*, *407*, 620–622.

Chervin, J. C., B. Canny, and M. Mancinelli (2001), Ruby-spheres as pressure gauge for optically transparent high pressure cells, *High Pressure Res.*, *21*, 305–314.

Daniel, I., H. Cardon, G. Fiquet, F. Guyot, and M. Mezouar (2001), Equation of state of Al-bearing perovskite to lower mantle pressure conditions, *Geophys. Res. Lett.*, *28*, 3789–3792.

Daniel, I., J. D. Bass, G. Fiquet, H. Cardon, J. Zhang, and M. Hanfland (2004), Effect of aluminum on the compressibility of silicate perovskite, *Geophys. Res. Lett.*, *31*, L15608, doi:10.1029/2004GL020213.

da Silva, C. R. S., R. M. Wentzcovitch, A. Patel, G. D. Price, and S. I. Karato (2000), The composition and geotherm of the lower mantle: Constraints from the elasticity of silicate perovskite, *Phys. Earth Planet. Inter.*, *118*, 103–109.

Davies, G. F., and A. M. Dziewonski (1975), Homogeneity and constitution of the Earth's lower mantle and outer core, *Phys. Earth Planet. Inter.*, *10*, 336–343.

Fiquet, G., A. Dewaele, D. Andrault, M. Kunz, and T. Le Bihan (2000), Thermoelastic properties and crystal structure of $MgSiO_3$ perovskite at lower mantle pressure and temperature conditions, *Geophys. Res. Lett.*, *27*, 21–24.

Grand, S. P., R. D. van der Hilst, and S. Widiyantoro (1997), Global seismic tomography: A snapshot of convection in the mantle, *GSA Today*, *7*, 1–7.

Irifune, T. (1994), Absence of an aluminous phase in the upper part of the Earth's lower mantle, *Nature*, *370*, 131–133.

Ishii, M., and J. Tromp (1999), Normal-mode and free-air gravity constraints on lateral variations in velocity and density of the Earth's mantle, *Science*, *285*, 1231–1236.

Jackson, J. M. (2005), The effect of minor elements on the physical and chemical properties of lower mantle minerals at high-pressure, Ph.D. thesis, Univ. of Ill., Urbana-Champaign.

Jackson, J. M., J. Zhang, and J. D. Bass (2004), Sound velocities and elasticity of aluminous $MgSiO_3$ perovskite: Implications for aluminum heterogeneity in Earth's lower mantle, *Geophys. Res. Lett.*, *31*, L10614, doi:10.1029/2004GL019918.

Kiefer, B., L. Stixrude, and R. Wentzcovitch (2002), Elasticity of (Mg, Fe)SiO_3-perovskite at high pressures, *Geophys. Res. Lett.*, *29*(11), 1539, doi:10.1029/2002GL014683.

Knittle, E., and R. Jeanloz (1987), Synthesis and equation of state of (Mg, Fe)SiO_3 perovskite to over 100 gigapascals, *Science*, *235*, 668–670.

Kubo, A., T. Tagi, S. Ono, and M. Akaogi (2000), Compressibility of $Mg_{0.9}A_{10.2}Si_{0.9}O_3$ perovskite, *Proc. Jpn. Acad., Ser. B*, *76*, 103–107.

Li, B., and J. Zhang (2005), Pressure and temperature dependence of elastic wave velocity of $MgSiO_3$ perovskite and the composition of the lower mantle, *Phys. Earth Planet. Inter.*, *151*, 143–154.

Mao, H.-K., J. Xu, and P. M. Bell (1986), Calibration of the ruby pressure gauge to 800-kbar under quasi-hydrostatic conditions, *J. Geophys. Res.*, *91*(B5), 4673–4676.

Masters, G., G. Laske, H. Bolton, and A. Dziewonski (2000), The relative behavior of shear velocity, bulk sound velocity and compressional velocity in the mantle: Implications for chemical and thermal structure, in *Earth's Deep Interior: Mineral Physics and Tomography From the Atomic to the Global Scale*, *Geophys. Monogr. Ser.*, vol. 117, edited by S. Karato et al., pp. 63–87, AGU, Washington, D. C.

Mattern, E., J. Matas, Y. Ricard, and J. Bass (2005), Lower mantle composition and temperature from mineral physics and thermodynamic modelling, *Geophys. J. Int.*, *160*, 973–990, doi:10.1111/j.1365-246X.2004.02549.x.

Ni, S., E. Tan, M. Gurnis, and D. Helmberger (2002), Sharp sides to the African superplume, *Science*, *296*, 1850–1852.

Ono, S., T. Kikegawa, and T. Iizuka (2005), The equation of state of orthorhombic perovskite in a peridotitic mantle composition to 80 GPa: Implication for chemical composition of the lower mantle, *Phys. Earth Planet. Inter.*, *145*, 9–17.

Sandercock, J. R. (1982), Trends in Brillouin scattering: Studies of opaque materials, supported films, and central modes, in *Topics in Applied Physics. Light Scattering in Solids III: Recent Results*, edited by M. Cardona and G. Guntherodt, pp. 173–206, Springer, New York.

Shim, S.-H., T. S. Duffy, and G. Shen (2000), The stability and P-V-T equation of state for $CaSiO_3$ perovskite in the earth's lower mantle, *J. Geophys. Res.*, *105*(B11), 25,955–25,968.

Sinelnikov, Y. D., G. Chen, D. R. Neuville, M. T. Vaughan, and R. C. Liebermann (1998), Ultrasonic shear wave velocities of $MgSiO_3$ perovskite at 8 GPa and 800 K and lower mantle composition, *Science*, *281*, 677–679.

Sinogeikin, S. V., T. Katsura, and J. D. Bass (1998), Sound velocities and elastic properties of Fe-bearing wadsleyite and ringwoodite, *J. Geophys. Res.*, *103*(B9), 20,819–20,825.

Sinogeikin, S. V., J. Zhang, and J. D. Bass (2004), Elasticity of single crystal and polycrystalline $MgSiO_3$ perovskite by Brillouin spectroscopy, *Geophys. Res. Lett.*, *31*, L06620, doi:10.1029/2004GL019559.

Trampert, J., F. Deschamps, J. Resovsky, and D. Yuen (2004), Probabilistic tomography maps: Chemical heterogeneities throughout the lower mantle, *Science*, *306*, 853–856.

Walter, M. J., A. Kubo, T. Yoshino, J. Brodholt, K. T. Koga, and Y. Ohishi (2004), Phase relations and equation-of-state of aluminous Mg-silicate perovskite and implications for Earth's lower mantle, *Earth Planet. Sci. Lett.*, *222*, 501–516.

Wentzcovitch, R. M., B. B. Karki, M. Cococcioni, and S. D. Gironcoli (2004), Thermoelastic properties of $MgSiO_3$-perovskite: Insights into the nature of the earth's lower mantle, *Phys. Rev. Lett.*, *92*, 01,8501.

Yagi, T., K. Okabe, N. Nishiyama, A. Kubo, and T. Kikegawa (2004), Complicated effects of aluminum on the compressibility of silicate perovskite, *Phys. Earth Planet. Inter.*, *143–144*, 81–89.

Yamamoto, T., D. A. Yuen, and T. Ebisuzaki (2003), Substitution mechanism of Al ions in $MgSiO_3$ perovskite under high pressure conditions from first-principles calculations, *Earth Planet. Sci. Lett.*, *206*, 617–625.

Zhang, J., and D. J. Weidner (1999), Thermal equation of state of aluminum-enriched silicate perovskite, *Science*, *284*, 782–784.

J. D. Bass and S. V. Sinogeikin, Department of Geology, University of Illinois, 1301 W. Green St., Urbana, IL 61801, USA.

J. M. Jackson, Advanced Photon Source, Argonne National Laboratory, 9700 S. Cass Avenue, Argonne, IL 60439, USA. (jjackson@aps.anl.gov)

J. Shu, Carnegie Institute of Washington, 5251 Broad Branch Road N.W., Washington, DC 20015, USA.

J. Zhang, Los Alamos National Laboratory, P.O. Box 1663, Los Alamos, NM 87545, USA.